Applied Bionics and Biomechanics 10 (2013) 41–58
DOI 10.3233/ABB-2012-0068
IOS Press

Slip effects on peristaltic transport in an inclined channel with mass transfer and chemical reaction

T. Hayat[a,*], Humaira Yasmin[a], S. Asghar[b] and Awatif A. Hendi[c]
[a]*Department of Mathematics, Quaid-I-Azam University, Islamabad, Pakistan*
[b]*Department of Mathematics, CIIT, Park Road Chak Shahzad, Islamabad, Pakistan*
[c]*Department of Physics, Faculty of Science, King Saud University, Riyadh, Saudi Arabia*

Abstract. An analysis is carried out for the peristaltic flow in an inclined asymmetric channel when no-slip condition does not hold. The whole analysis has been carried out in the presence of mass transfer and chemical reaction. The channel asymmetry is generated because of peristaltic wave train on the walls through different amplitudes and phases. Long wavelength and low Reynolds number assumption is adopted in the whole mathematical analysis. Expressions for the stream function and longitudinal pressure gradient have been developed. Numerical integration is performed for the analysis of pressure rise per wavelength. Longitudinal velocity, pumping and trapping phenomena are analyzed in detail via plots.

Keywords: Slip condition, nonlinear analysis and inclined asymmetric channel

1. Introduction

Peristaltic flows have attracted the recent researchers because of their relevance in many engineering and physiological processes. To be more specific such processes include urine transport from kidney to bladder, chyme movement in the gastrointestinal tract, food stuffs through esophagus, spermatozoa in the ductus afferents of male reproductive tract, vasomotion of small blood vessels etc.

The peristaltic flows also have indispensable role in heart lung machines, sanitary and corrosive fluids transport and locomotion. Latham [1] carried out the experimental work on peristaltic transport initially. Since then a rather ample literature is dedicated to peristaltic flows under various aspects. Kothandapani and Srinivas [2] have discussed the peristaltic transport of Jeffrey fluid under the effect of magnetic field in an asymmetric channel. In ref. [3], they discussed the effects of heat and mass transfer on peristaltic flow with compliant walls. Abd elmaboud and Mekheimer [4] studied the peristaltic motion of second order fluid in a porous medium. Mekheimer and Abd elmaboud [5] examined the endoscopic effects on the peristalsis of couple stress fluid. Effect of heat transfer on the MHD peristaltic flow of Newtonian fluid in a vertical annulus was studied by Mekheimer and Abd elmaboud [6]. The blood flow in a tapered artery in the presence of chemical reaction is investigated by Nadeem and Akbar [7]. The peristaltic flow of fourth grade fluid in the presence of magnetic field is analyzed by Hayat et al. [8]. Hayat and Abbasi [9] described the peristaltic flow with variable viscosity. Tripathi et al. [10] examined the peristaltic flow of fractional viscoelastic

*Corresponding author: T. Hayat, Department of Mathematics, Quaid-I-Azam University 45320, Islamabad 44000, Pakistan. Tel.: + 92 51 90642172; E-mail: pensy_t@yahoo.com.

fluid. Pandy and Tripathi [11] analyzed the influence of magnetic field on the peristaltic flow of viscous fluid in a finite length cylindrical tube. Peristaltic flow in an inclined channel with slip effect is described by Srinivas and Muthuraj [12]. Ali et al. [13] pointed out the slip effects on the peristalsis in MHD viscous fluid having variable viscosity. The peristaltic flow of Jeffrey fluid in an asymmetric channel with slip and induced magnetic field is studied by Nadeem and Akram [14]. Hayat et al. [15] examined the influence of heat transfer on the peristaltic flow with slip condition. Note that the slip flow is significant when the fluid has adhesion loss at the wetted wall making the fluid slide along the wall. Derek et al. [16] have experimentally shown that the fluid possesses non-continuum features such as slip flow when the molecular mean free path length of the fluid is comparable to the distance between the plates as in nanochannels/microchannels [17].

The present paper discusses the peristaltic flow of fourth grade fluid in an inclined asymmetric channel with mass transfer and chemical reaction. Analysis has been carried out in the presence of slip condition. In fact, the processes with mass transfer and chemical reaction effects are quite significant in chemical equipment. The mass transfer has indispensable role in several industrial applications including the polymer production and manufacturing of ceramics/glassware. In view of such motivation, the present study is arranged as follows. Next section deals with the problem statement. Solution of the arising nonlinear problem is presented in section three for small Deborah number and long wavelength analysis. Results and discussion are given in section four whereas section five consists of main conclusions.

2. Governing problem

Consider peristaltic flow of an incompressible fourth grade fluid through an asymmetric channel inclined at an angle α to the horizontal (see Fig. 1). We select $\bar{X}$ and $\bar{Y}$ axes along and perpendicular to the channel walls respectively. The flow induced is because of sinusoidal waves propagating with speed c. The wave shapes are

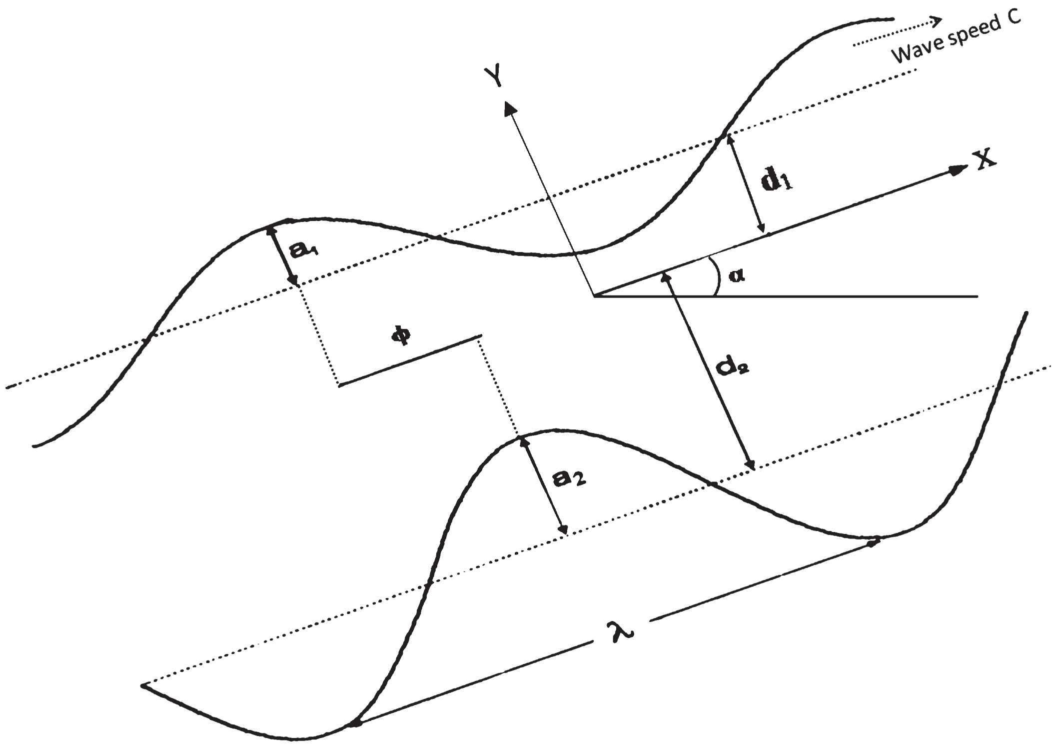

Fig. 1. Geometry of the problem.

$$\bar{H}_1(\bar{X},\bar{t}) = d_1 + a_1 \sin \frac{2\pi}{\lambda}(\bar{X} - c\bar{t}), \text{ upper wall},$$
$$\bar{H}_2(\bar{X},\bar{t}) = -d_2 - a_2 \sin \left(\frac{2\pi}{\lambda}(\bar{X} - c\bar{t}) + \phi\right), \text{ lower wall}. \quad (1)$$

In above expressions $a_i (i = 1, 2)$ are the wave amplitudes, λ the wavelength, $d_1 + d_2$ is the width of the channel, the phase difference ϕ varies in the range $0 \leq \phi \leq \pi$ ($\phi = 0$ corresponds to symmetric channel with waves out of phase and $\phi = \pi$ the waves are in phase) and further $a_1,\ a_2,\ d_1,\ d_2$ and ϕ obey the following relation

$$a_1^2 + a_2^2 + 2a_1a_2 \cos\phi \leq (d_1 + d_2)^2. \quad (2)$$

We further have C_1 and C_0 as the respective concentration fields at the lower and upper walls respectively.

The flow situation in absence of body forces can be described by the following equations

$$\text{div}\,\bar{\mathbf{V}} = 0, \quad (3)$$

$$\rho\frac{d\bar{\mathbf{V}}}{d\bar{t}} = -\text{grad}\,\bar{p} + \text{div}\,\bar{\mathbf{S}}, \quad (4)$$

$$\frac{\partial C}{\partial \bar{t}} + \bar{U}\frac{\partial C}{\partial \bar{X}} + \bar{V}\frac{\partial C}{\partial \bar{Y}} = D\left[\frac{\partial^2 C}{\partial \bar{X}^2} + \frac{\partial^2 C}{\partial \bar{Y}^2}\right] - k_1 C, \quad (5)$$

where $\bar{\mathbf{V}}$ is the velocity, C the concentration of the fluid, $\bar{p}$ the pressure, ρ density of the fluid, $\frac{d}{dt}$ is the material time derivative, $\bar{\mathbf{S}}$ the extra stress tensor, D the concentration parameter, k_1 the chemical reaction parameter and bar refers the dimensional quantity.

The velocity $\bar{\mathbf{V}}$ and extra stress tensor $\bar{\mathbf{S}}$ in a fourth grade fluid can be written as

$$\bar{\mathbf{V}} = (\bar{U}(\bar{X},\bar{Y},\bar{t}), \bar{V}(\bar{X},\bar{Y},\bar{t}), 0), \quad (6)$$

$$\begin{aligned}\bar{\mathbf{S}} = {}& \mu\bar{\mathbf{A}}_1 + \alpha_1\bar{\mathbf{A}}_2 + \alpha_2\bar{\mathbf{A}}_1^2 + \beta_1\bar{\mathbf{A}}_3 + \beta_2(\bar{\mathbf{A}}_2\bar{\mathbf{A}}_1 + \bar{\mathbf{A}}_1\bar{\mathbf{A}}_2)\\ &+ \beta_3(tr\bar{\mathbf{A}}_1^2)\bar{\mathbf{A}}_1 + \gamma_1\bar{\mathbf{A}}_4 + \gamma_2(\bar{\mathbf{A}}_3\bar{\mathbf{A}}_1 + \bar{\mathbf{A}}_1\bar{\mathbf{A}}_3) + \gamma_3\bar{\mathbf{A}}_2^2\\ &+ \gamma_4(\bar{\mathbf{A}}_2\bar{\mathbf{A}}_1^2 + \bar{\mathbf{A}}_1^2\bar{\mathbf{A}}_2) + \gamma_5(tr\bar{\mathbf{A}}_2)\bar{\mathbf{A}}_2 + \gamma_6(tr\bar{\mathbf{A}}_2)\bar{\mathbf{A}}_1^2\\ &+ [\gamma_7 tr\bar{\mathbf{A}}_3 + \gamma_8 tr(\bar{\mathbf{A}}_2\bar{\mathbf{A}}_1)]\bar{\mathbf{A}}_1, \end{aligned} \quad (7)$$

where μ denotes the coefficient of shear viscosity and $\alpha_i (i = 1, 2)$, $\beta_j (j = 1 - 3)$, $\gamma_k (k = 1 - 8)$ are the material constants. When γ_k's are zero then we have the third grade fluid. For β_j's and γ_k's equal to zero, we get the expression for second grade fluid and $\alpha_i = \beta_j = \gamma_k = 0$ corresponds to the viscous fluid case.

The definition of Rivlin-Ericksen tensors are as follows:

$$\bar{\mathbf{A}}_1 = (\text{grad}\,\bar{\mathbf{V}}) + (\text{grad}\,\bar{\mathbf{V}})^T,$$
$$\bar{\mathbf{A}}_n = \frac{d\bar{\mathbf{A}}_{n-1}}{dt} + \bar{\mathbf{A}}_{n-1}(\text{grad}\,\bar{\mathbf{V}}) + (\text{grad}\,\bar{\mathbf{V}})^T\bar{\mathbf{A}}_{n-1}, n > 1. \quad (8)$$

If $(\bar{U}, \bar{V})$ and $(\bar{u}, \bar{v})$ are the velocity components in the laboratory and wave frames then the relations between these frames are

$$\bar{x} = \bar{X} - c\bar{t}, \bar{y} = \bar{Y}, \bar{u}(\bar{x},\bar{y}) = \bar{U}(\bar{X},\bar{Y},\bar{t}) - c, \bar{v}(\bar{x},\bar{y}) = \bar{V}(\bar{X},\bar{Y},\bar{t}). \quad (9)$$

Using above transformations and introducing the following dimensionless variables

$$x = \frac{2\pi\bar{x}}{\lambda},\ y = \frac{\bar{y}}{d_1},\ u = \frac{\bar{u}}{c},\ v = \frac{\bar{v}}{c},\ \ p = \frac{2\pi d_1^2\bar{p}}{c\mu\lambda},$$
$$h_1 = \frac{\bar{h}_1}{d_1},\ h_2 = \frac{\bar{h}_2}{d_1},\ \ t = \frac{2\pi c\bar{t}}{\lambda}, \mathbf{S} = \frac{d_1}{\mu c}\bar{\mathbf{S}},\ \sigma = \frac{C - C_0}{C_1 - C_0}, \quad (10)$$

we obtain

$$\delta \operatorname{Re}\left[\left(\frac{\partial\psi}{\partial y}\frac{\partial}{\partial x}-\frac{\partial\psi}{\partial x}\frac{\partial}{\partial y}\right)\left(\frac{\partial\psi}{\partial y}\right)\right]+\frac{\partial p}{\partial x}=\delta\frac{\partial S_{xx}}{\partial x}+\frac{\partial S_{xy}}{\partial y}+\frac{\operatorname{Re}\sin\alpha}{Fr}, \tag{11}$$

$$-\delta^3 \operatorname{Re}\left[\left(\frac{\partial\psi}{\partial y}\frac{\partial}{\partial x}-\frac{\partial\psi}{\partial x}\frac{\partial}{\partial y}\right)\left(\frac{\partial\psi}{\partial x}\right)\right]+\frac{\partial p}{\partial y}=\delta^2\frac{\partial S_{xy}}{\partial x}+\delta\frac{\partial S_{yy}}{\partial y}-\delta\frac{\operatorname{Re}\cos\alpha}{Fr}, \tag{12}$$

$$\operatorname{Re}\delta\left[\left(\frac{\partial\psi}{\partial y}\frac{\partial}{\partial x}-\frac{\partial\psi}{\partial x}\frac{\partial}{\partial y}\right)\sigma\right]=\frac{1}{Sc}\left[\delta^2\frac{\partial^2}{\partial x^2}+\frac{\partial^2}{\partial y^2}\right]\sigma-\gamma\sigma-C^*, \tag{13}$$

where continuity equation is automatically satisfied and

$$\begin{aligned}\mathbf{S}=&\ \mathbf{A}_1+\lambda_1\mathbf{A}_2+\lambda_2\mathbf{A}_1^2+\xi_1\mathbf{A}_3+\xi_2(\mathbf{A}_2\mathbf{A}_1+\mathbf{A}_1\mathbf{A}_2)\\&+\xi_3(tr\mathbf{A}_1^2)\mathbf{A}_1+\eta_1\mathbf{A}_4+\eta_2(\mathbf{A}_3\mathbf{A}_1+\mathbf{A}_1\mathbf{A}_3)+\eta_3\mathbf{A}_2^2\\&+\eta_4(\mathbf{A}_2\mathbf{A}_1^2+\mathbf{A}_1^2\mathbf{A}_2)+\eta_5(tr\mathbf{A}_2)\mathbf{A}_2+\eta_6(tr\mathbf{A}_2)\mathbf{A}_1^2\\&+[\eta_7 tr\mathbf{A}_3+\eta_8 tr(\mathbf{A}_2\mathbf{A}_1)]\mathbf{A}_1.\end{aligned} \tag{14}$$

In the above equations $u=\frac{\partial\psi}{\partial y},\ v=-\delta\frac{\partial\psi}{\partial x}$, with ψ as the stream function. Further, the wave number (δ), the Reynolds number (Re), the Froud number (Fr), the Schmidt number (Sc), the chemical reaction parameter (γ) and the dimensionless material parameters $\lambda_i(i=1,2)$, $\xi_j(j=1-3)$, $\eta_k(k=1-8)$ are

$$\begin{aligned}&\delta=\frac{2\pi d_1}{\lambda},\operatorname{Re}=\frac{\rho c d_1}{\mu},\ Fr=\frac{c^2}{g d_1},\ Sc=\frac{\mu}{\rho D},\\&\gamma=\frac{\rho k_1 d_1^2}{\mu},\lambda_1=\frac{\alpha_1 c}{\mu d_1},\lambda_2=\frac{\alpha_2 c}{\mu d_1},\xi_1=\frac{\beta_1 c^2}{\mu d_1^2},\\&\xi_2=\frac{\beta_2 c^2}{\mu d_1^2},\xi_3=\frac{\beta_3 c^2}{\mu d_1^2},\eta_1=\frac{\gamma_1 c^3}{\mu d_1^3},\eta_2=\frac{\gamma_2 c^3}{\mu d_1^3},\\&\eta_3=\frac{\gamma_3 c^3}{\mu d_1^3},\eta_4=\frac{\gamma_4 c^3}{\mu d_1^3},\eta_5=\frac{\gamma_5 c^3}{\mu d_1^3},\eta_6=\frac{\gamma_6 c^3}{\mu d_1^3},\\&\eta_7=\frac{\gamma_7 c^3}{\mu d_1^3},\eta_8=\frac{\gamma_8 c^3}{\mu d_1^3},\end{aligned} \tag{15}$$

with $C^*=\frac{\rho k_1 C_0 d_1^2}{\mu(C_1-C_0)}$.

From Equations. (11 and 12) we can write

$$\delta \operatorname{Re}\left[\left(\frac{\partial\psi}{\partial y}\frac{\partial}{\partial x}-\frac{\partial\psi}{\partial x}\frac{\partial}{\partial y}\right)\nabla^2\psi\right]=\left[\left(\frac{\partial^2}{\partial y^2}-\delta^2\frac{\partial^2}{\partial x^2}\right)S_{xy}\right]+\delta\left[\frac{\partial^2}{\partial x\partial y}(S_{xx}-S_{yy})\right], \tag{16}$$

in which

$$\nabla^2=\left(\delta^2\frac{\partial^2}{\partial x^2}+\frac{\partial^2}{\partial y^2}\right). \tag{17}$$

The dimensional volume flow rate in fixed frame is defined by the following expression

$$Q=\int_{\bar{h}_2(\bar{X},\bar{t})}^{\bar{h}_1(\bar{X},\bar{t})}\bar{U}(\bar{X},\bar{Y},\bar{t})d\bar{Y}. \tag{18}$$

The above expression in wave frame reduces to

$$q=\int_{\bar{h}_2(\bar{x})}^{\bar{h}_1(\bar{x})}\bar{u}(\bar{x},\bar{y})d\bar{y}. \tag{19}$$

Moreover Equations (9, 18 and 19) give

$$Q=q+c\bar{h}_1(\bar{x})-c\bar{h}_2(\bar{x}). \tag{20}$$

The time-mean flow over a period T is defined by

$$\bar{Q}=\frac{1}{T}\int_0^T Q d\bar{t}. \tag{21}$$

Invoking Equation (20) into Equation (21) and then performing integration we can express that

$$\bar{Q}=q+cd_1+cd_2. \tag{22}$$

Introducing the dimensionless mean flow rates θ (in fixed frame) and F (in laboratory frame) by the relations

$$\theta = \frac{\bar{Q}}{cd_1}, \quad F = \frac{q}{cd_1}, \tag{23}$$

we get from Equation (22) the following expression

$$\theta = F + 1 + d, \tag{24}$$

where

$$F = \int_{h_2(x)}^{h_1(x)} \frac{\partial \psi}{\partial y} dy = \psi(h_1(x)) - \psi(h_2(x)), \tag{25}$$

and the dimensionless forms of h_i $(i = 1,\ 2)$ are

$$h_1(x) = 1 + a\sin(x), \quad h_2(x) = -d - b\sin(x + \phi), \tag{26}$$

with $a = a_1/d_1$, $b = a_2/d_1$, $d = d_2/d_1$ and ϕ satisfies the following relation

$$a^2 + b^2 + 2ab\cos\phi \leq (1 + d)^2. \tag{27}$$

The dimensionless slip conditions in wave frame are

$$\psi = \frac{F}{2}, \ \ \frac{\partial \psi}{\partial y} + \beta S_{xy} = -1, \ \sigma + \beta_1 \frac{\partial \sigma}{\partial y} = 0, \quad \text{at } y = h_1(x),$$
$$\psi = -\frac{F}{2}, \ \ \frac{\partial \psi}{\partial y} - \beta S_{xy} = -1, \ \sigma - \beta_1 \frac{\partial \sigma}{\partial y} = 1, \quad \text{at } y = h_2(x), \tag{28}$$

where $\beta \left(= \mu\bar{\beta}/d_1\right)$ and $\beta_1 \left(= \mu\bar{\beta}_1/d_1\right)$ are the dimensionless velocity and concentration slip parameters, $\bar{\beta}$ and $\bar{\beta}_1$ are the dimensional velocity and concentration slip parameters and S_{xy} is given through Equation (14). The resulting problem after adopting long wavelength and low Reynolds number procedure becomes:

$$\frac{\partial^2 S_{xy}}{\partial y^2} = 0, \tag{29}$$

$$\frac{dp}{dx} = \frac{\partial S_{xy}}{\partial y} + \frac{\mathrm{Re}\sin\alpha}{Fr}, \tag{30}$$

$$\frac{1}{Sc}\left(\frac{\partial^2 \sigma}{\partial y^2}\right) - \gamma\sigma - C^* = 0, \tag{31}$$

with

$$S_{xy} = \frac{\partial^2 \psi}{\partial y^2} + 2\Gamma\left(\frac{\partial^2 \psi}{\partial y^2}\right)^3 \tag{32}$$

in which $\Gamma(= \xi_2 + \xi_3)$ is the Deborah number and $p \neq p(y)$.

3. Solution methodology

Obviously the governing flow Equations (29 and 30) are nonlinear even after using long wavelength approximation. Further, the velocity slip boundary conditions are nonlinear whereas such conditions are linear in absence of slip parameter $(\beta = 0)$. Closed form solution even in case of no-slip situation is not available. We intend here to find the series solution for small Deborah number Γ. Hence we expand the flow quantities as follows:

$$\psi = \psi_0 + \Gamma\psi_1 + \Gamma^2\psi_2 + ...,$$
$$p = p_0 + \Gamma p_1 + \Gamma^2 p_2 + ...,$$
$$F = F_0 + \Gamma F_1 + \Gamma^2 F_2 + ... \tag{33}$$

Putting above expressions into Equations (29, 30 and 32) and then separating the coefficients of like powers of Γ we get systems of different orders. Solving the resulting systems up to $O(\Gamma^2)$ we have

$$\psi_0 = R_1 y^3 + R_2 y^2 + R_3 y + R_4, \tag{34}$$

$$\psi_1 = M_1 y^5 + M_2 y^4 + M_3 y^3 + M_4 y^2 + M_5 y + M_6, \tag{35}$$

$$\psi_2 = N_1 y^7 + N_2 y^6 + N_3 y^5 + N_4 y^4 + N_5 y^3 + N_6 y^2 + N_7 y + N_8, \tag{36}$$

$$u_0 = 3R_1 y^2 + 2R_2 y + R_3, \tag{37}$$

$$u_1 = 5M_1 y^4 + 4M_2 y^3 + 3M_3 y^2 + 2M_4 y + M_5, \tag{38}$$

$$u_2 = 7N_1 y^6 + 6N_2 y^5 + 5N_3 y^4 + 4N_4 y^3 + 3N_5 y^2 + 2N_6 y + N_7, \tag{39}$$

$$\frac{dp_0}{dx} = \frac{-12(F_0 + h_1 - h_2)}{(h_1 - h_2)^2(h_1 - h_2 + 6\beta)} + 12G, \tag{40}$$

$$\frac{dp_1}{dx} = \frac{-60F_1 + \left(\frac{dp_0}{dx} - 12G\right)^3 L_{19} + \left(\frac{dp_0}{dx} - 12G\right)^2 R_2 L_{20} + \left(\frac{dp_0}{dx} - 12G\right) S_2^2 L_{21}}{5(h_1 - h_2)^2 (h_1 - h_2 + 6\beta)}, \tag{41}$$

$$\frac{dp_2}{dx} = \frac{-420F_2 + \left(\frac{dp_0}{dx} - 12G\right)^2 L_{37} + \left(\frac{dp_0}{dx} - 12G\right) S_2 L_{38} + S_2^2 L_{39}}{35(h_1 - h_2)^2 (h_1 - h_2 + 6\beta)}, \tag{42}$$

where $G = (\text{Re} \sin\alpha)/(12\ Fr)$ and the different quantities appearing in the above expressions have been presented in the Appendix A.

The non-dimensional pressure rise per wavelength at zeroth, first and second orders are

$$\Delta P_{\lambda_0} = \int_0^{2\pi} \frac{dp_0}{dx} dx,\ \Delta P_{\lambda_1} = \int_0^{2\pi} \frac{dp_1}{dx} dx,\ \Delta P_{\lambda_2} = \int_0^{2\pi} \frac{dp_2}{dx} dx. \tag{43}$$

The perturbation expressions of ψ, ΔP_λ and dp/dx upto $O(\Gamma^2)$ are denoted by $\psi^{(2)}$, $\Delta P_\lambda^{(2)}$and $dp^{(2)}/dx$. These can be written as

$$\psi^{(2)} = \psi_0 + \Gamma\psi_1 + \Gamma^2\psi_2. \tag{44}$$

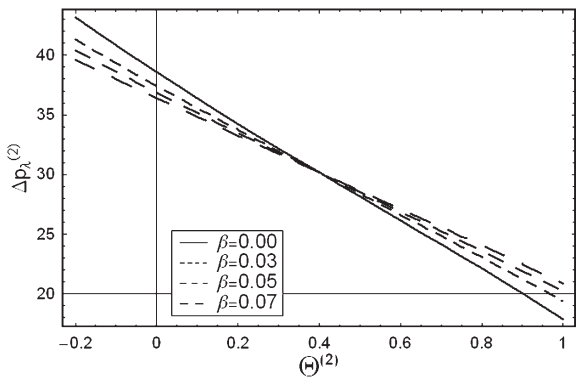

Fig. 2. Effect of slip parameter β on variation of $\Delta p_\lambda^{(2)}$ with $\theta^{(2)}$ for $a = 0.2, b = 0.5, d = 0.8, \text{Re} = 10, \Gamma = 0.01, Fr = 1, \sin\alpha = 0.5$ and $\phi = \pi/4$.

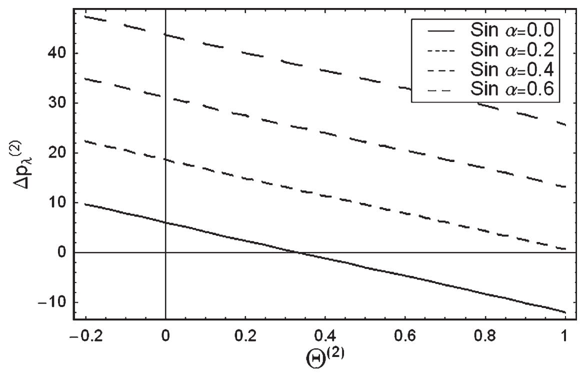

Fig. 4. Effect of inclined angle α on variation of $\Delta p_\lambda^{(2)}$ with $\theta^{(2)}$ for $a = 0.2, b = 0.5, d = 0.7, \text{Re} = 10, \Gamma = 0.04, Fr = 1, \beta = 0.1$ and $\phi = \pi/4$.

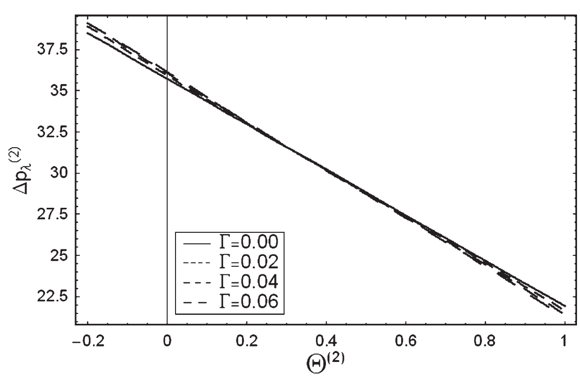

Fig. 3. Effect of Deborah number Γ on variation of $\Delta p_\lambda^{(2)}$ with $\theta^{(2)}$ for $a = 0.2$, $b = 0.5$, $d = 0.8$, $\text{Re} = 10$, $\beta = 0.1$, $Fr = 1$, $\sin\alpha = 0.5$ and $\phi = \pi/4$.

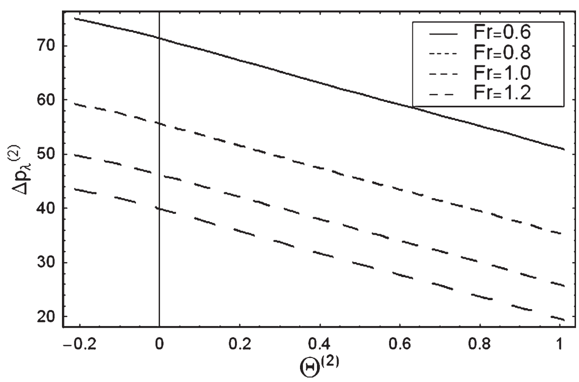

Fig. 5. Effect of Froud number Fr on variation of $\Delta p_\lambda^{(2)}$ with $\theta^{(2)}$ for $a = 0.3, b = 0.5, d = 0.7, \text{Re} = 10, \Gamma = 0.04, \beta = 0.1, \sin\alpha = 0.6$ and $\phi = \pi/4$.

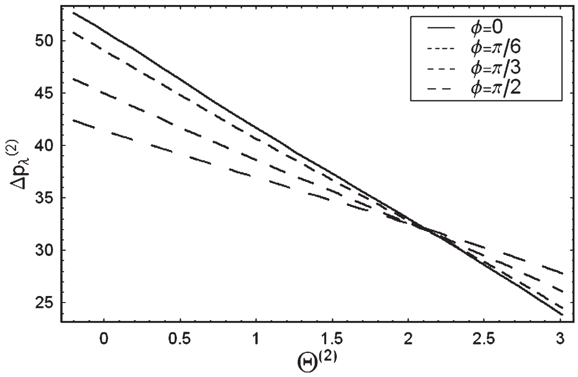

Fig. 6. Effect of phase difference ϕ on variation of $\Delta p_{\lambda}^{(2)}$ with $\theta^{(2)}$ for $a = 0.7$, $b = 1.2$, $d = 2$, $\mathrm{Re} = 10$, $\Gamma = 0.01$, $\beta = 0.1$, $\sin\alpha = 0.6$ and $Fr = 1$.

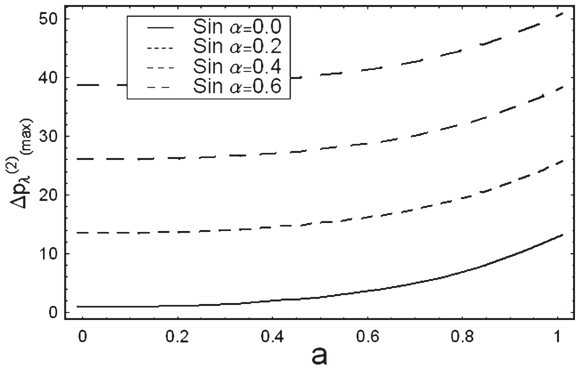

Fig. 9. Effect of inclined angle α on variation of $\Delta p_{\lambda(\max)}^{(2)}$ with a for $\theta = 0.0001$, $b = 0.4$, $d = 1$, $\mathrm{Re} = 10$, $\Gamma = 0.02$, $Fr = 1$, $\beta = 0.1$ and $\phi = \pi/2$.

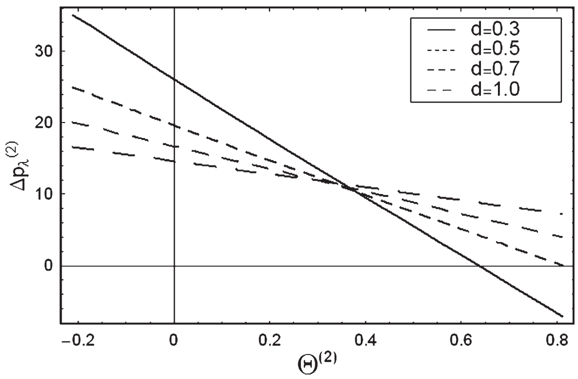

Fig. 7. Effect of width of the channel d on variation of $\Delta p_{\lambda}^{(2)}$ with $\theta^{(2)}$ for $a = 0.2$, $b = 0.4$, $\phi = \pi/6$, $\mathrm{Re} = 10$, $\Gamma = 0.01$, $\beta = 0.1$, $\sin\alpha = 0.2$ and $Fr = 1$.

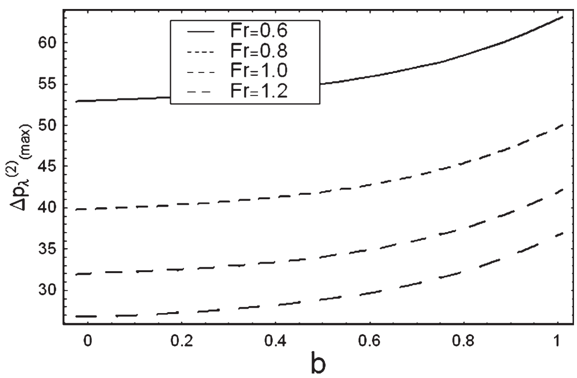

Fig. 10. Effect of Froud number Fr on variation of $\Delta p_{\lambda(\max)}^{(2)}$ with b for $a = 0.5$, $\theta = 0.0001$, $d = 1.5$, $\mathrm{Re} = 10$, $\Gamma = 0.02$, $\beta = 0.1$, $\sin\alpha = 0.2$ and $\phi = \pi/4$.

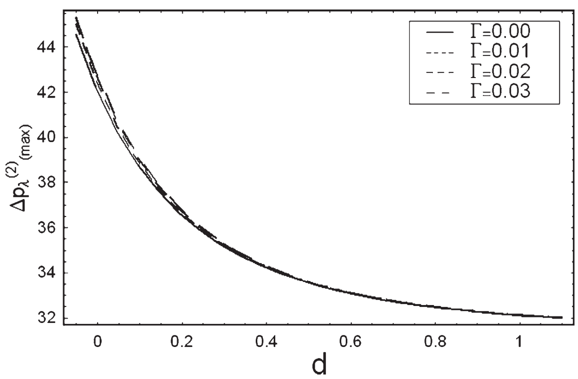

Fig. 8. Effect of Deborah number Γ on variation of $\Delta p_{\lambda(\max)}^{(2)}$ with d for $a = 0.3$, $b = 0.2$, $\theta = -0.001$, $\mathrm{Re} = 10$, $\beta = 0.1$, $Fr = 1$, $\sin\alpha = 0.2$ and $\phi = \pi/2$.

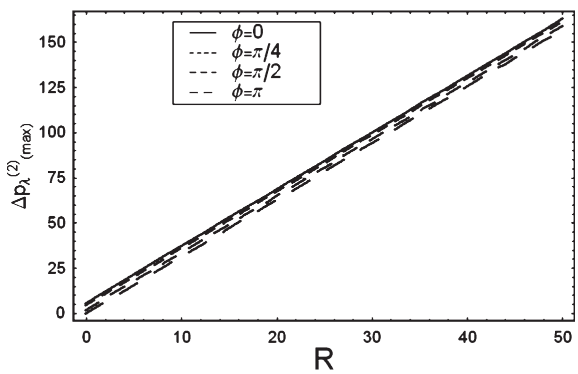

Fig. 11. Effect of phase difference ϕ on variation of $\Delta p_{\lambda(\max)}^{(2)}$ with Re for $a = 0.5$, $b = 0.7$, $d = 1.5$, $\theta = 0.0001$, $\Gamma = 0.02$, $\beta = 0.1$, $\sin\alpha = 0.2$ and $Fr = 1$.

$$\Delta P_{\lambda}^{(2)} = \Delta P_{\lambda_0} + \Gamma \Delta P_{\lambda_1} + \Gamma^2 \Delta P_{\lambda_2}. \tag{45}$$

$$\frac{dp^{(2)}}{dx} = \frac{dp_0}{dx} + \Gamma \frac{dp_1}{dx} + \Gamma^2 \frac{dp_2}{dx}. \tag{46}$$

It is worth pointing to note that solution expression for zeroth order system are similar to that of viscous fluid. Further, the results coincide with that of no-slip condition when $\beta = 0$. Now the solution of Equations (28 and 31) is

$$\begin{aligned}\sigma(y) = \Big[& e^{-\sqrt{Sc*\gamma}y} \Big\{ C^* \Big(e^{(h_1+2h_2)\sqrt{Sc*\gamma}}(1 - \beta_1\sqrt{Sc*\gamma}) + e^{\sqrt{Sc*\gamma}(h_2+2y)}(1 - \beta_1\sqrt{Sc*\gamma}) \\ & - e^{(2h_2+y)\sqrt{Sc*\gamma}}(-1 + \beta_1\sqrt{Sc*\gamma})^2 - (e^{(2h_1+h_2)\sqrt{Sc*\gamma}} + e^{(h_1+2y)\sqrt{Sc*\gamma}}) \\ & *(1 + \beta_1\sqrt{Sc*\gamma}) + e^{(2h_1+y)\sqrt{Sc*\gamma}}(1 + \beta_1\sqrt{Sc*\gamma})^2 \Big) \\ & - e^{(h_1+2y)\sqrt{Sc*\gamma}}(1 + \beta_1\sqrt{Sc*\gamma})\gamma + e^{(h_1+2h_2)\sqrt{Sc*\gamma}}(1 + \beta_1\sqrt{Sc*\gamma})\gamma \Big\} \Big] \\ & / \Big[\gamma \Big\{ e^{2h_2\sqrt{Sc*\gamma}}(-1 + \beta_1\sqrt{Sc*\gamma})^2 - e^{2h_2\sqrt{Sc*\gamma}}(1 + \beta_1\sqrt{Sc*\gamma})^2 \Big\} \Big]\end{aligned} \tag{47}$$

4. Results and discussion

4.1. Pumping characteristics

Our intention in this subsection is to discuss the behaviors of pressure rise and streamlines for embedded flow parameters. Note that the definition of pressure rise involves integration of $dp^{(2)}/dx$. The arising integral is not solvable analytically. Hence **MATHEMATICA** is used to perform the integration. The variations of $\Delta p_{\lambda}^{(2)}$ against the flow rate $\theta^{(2)}$ for fixed values of involved parameters have been sketched in the Figs. 2–7. Figure 2 represents the variation of dimensionless pressure rise up to second order ($\Delta p_{\lambda}^{(2)}$) with the second order dimensionless mean flow rate ($\theta^{(2)}$) for various values of β. This figure illustrates that peristaltic pumping rate decreases by increasing β. It is interesting to note that in copumping the pumping rate increases by increasing β. Figure 3 displays the dimensionless pressure gradient to second-order $\Delta p_{\lambda}^{(2)}$ for different values of Deborah number Γ. A linear relationship is noticed between the pressure gradient and the flow rate in a viscous fluid i.e. when $\Gamma = 0$. As expected the pumping curves are non-linear when $\Gamma \neq 0$. Therefore, for $\Delta p_{\lambda}^{(2)} > 30$, increasing Γ gives a better pumping performance and for $\Delta p_{\lambda}^{(2)} = 30$, there is no difference between the viscous and fourth-grade fluids on pumping as the pumping curves coincide with each other.

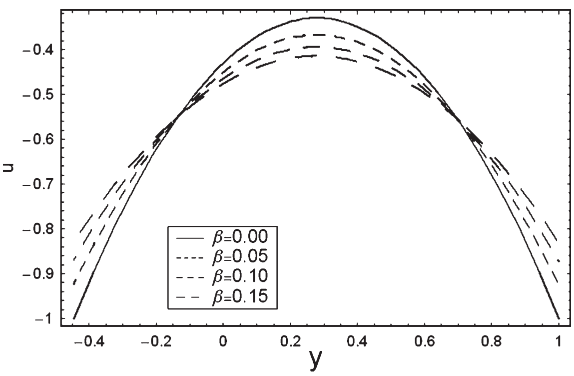

Fig. 12. Effect of slip parameter β on the variation of longitudinal velocity u plotted for $a = 0.2$, $b = 0.5$, $d = 0.8$, $\Gamma = 0.01$, $\theta = 1$, $x = \pi$, $\alpha = \pi/6$, Re $= 0.5$, $Fr = 1$, $dp^{(2)}/dx = 1$ and $\phi = \pi/4$.

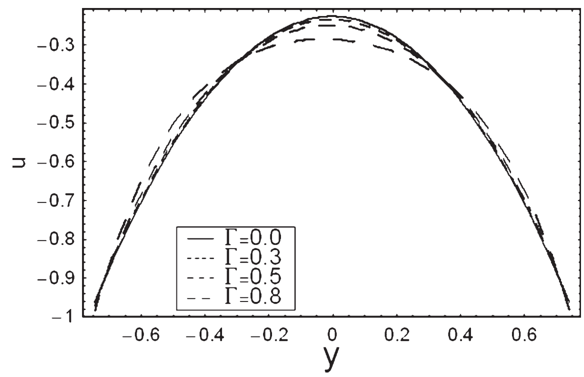

Fig. 13. Effect of the Deborah number Γ on the variation of longitudinal velocity u plotted for $a = 0.3$, $b = 0.6$, $d = 0.9$, Re $= 1.5$, $\phi = \pi/4$, $Fr = 1.1$, $\alpha = \pi/6$, $\theta = 1.2$, $x = -\pi/3$, $\beta = 0.02$ and $dp^{(2)}/dx = 1$.

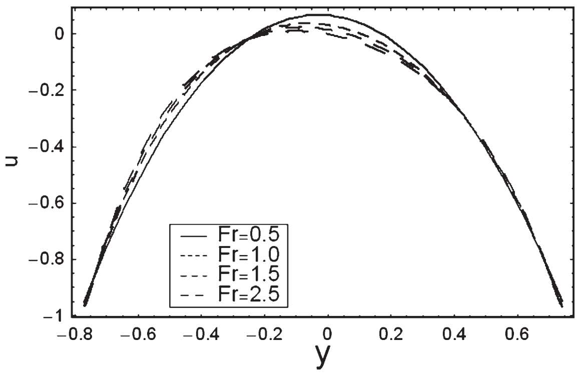

Fig. 14. Effect of the Froud number Fr on the variation of longitudinal velocity u plotted for $a = 0.3$, $b = 0.5$, $d = 0.9$, $\mathrm{Re} = 0.7$, $\phi = \pi/4$, $\Gamma = 0.15$, $\alpha = \pi/6$, $\theta = 1.5$, $x = -\pi/3$, $\beta = 0.02$ and $dp^{(2)}/dx = 1$.

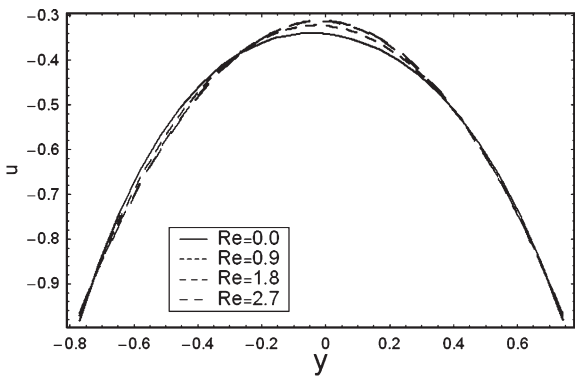

Fig. 15. Effect of the Reynold number Re on the variation of longitudinal velocity u plotted for $a = 0.3$, $b = 0.5$, $d = 0.9$, $Fr = 1.2$, $\phi = \pi/4$, $\Gamma = 0.2$, $\alpha = \pi/6$, $\theta = 1.1$, $x = -\pi/3$, $\beta = 0.02$ and $dp^{(2)}/dx = 1$.

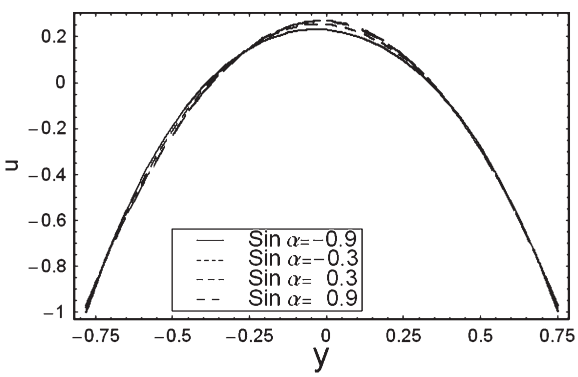

Fig. 16. Effect of $\sin\alpha$ on the variation of longitudinal velocity u plotted for $a = 0.3$, $b = 0.5$, $d = 0.9$, $Fr = 1.3$, $\phi = \pi/4$, $\Gamma = 0.03$, $\mathrm{Re} = 2$, $\theta = 1.5$, $x = -\pi/3$, $\beta = 0.02$ and $dp^{(2)}/dx = 1$.

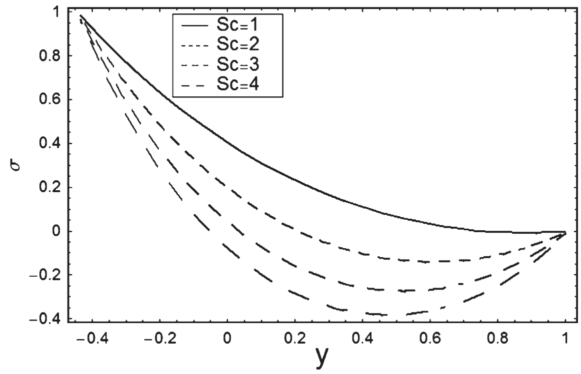

Fig. 17. Variation of Sc on σ when $a = 0.2$, $b = 0.8$, $d = 1$, $\beta_1 = 0.01$, $\phi = \pi/4$, $x = \pi$, $C^* = 1$, $\gamma = 1$.

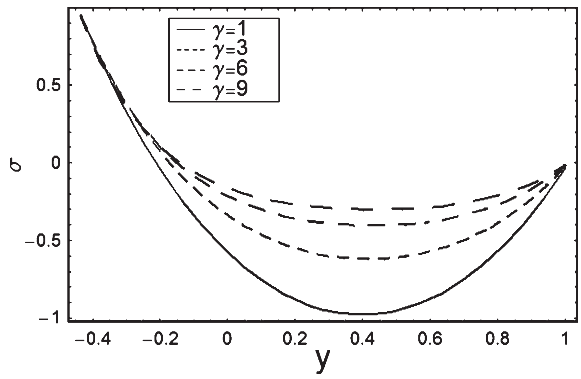

Fig. 18. Variation of γ on σ when $a = 0.2$, $b = 0.8$, $d = 1$, $\beta_1 = 0.01$, $\phi = \pi/4$, $x = \pi$, $C^* = 3.2$, $Sc = 2.2$.

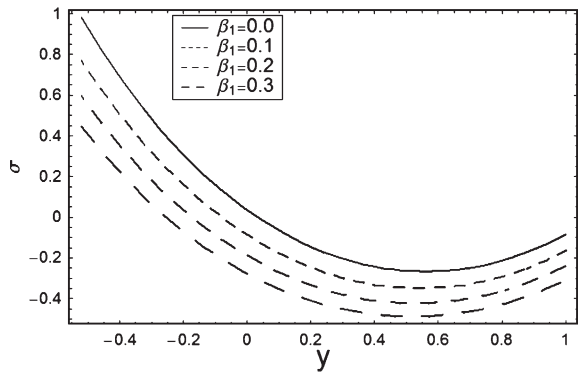

Fig. 19. Variation of β_1 on σ when $a = 0.2$, $b = 0.8$, $d = 1$, $Sc = 1.5$, $\phi = \pi/4$, $x = \pi$, $C^* = 1.5$, $\gamma = 1$.

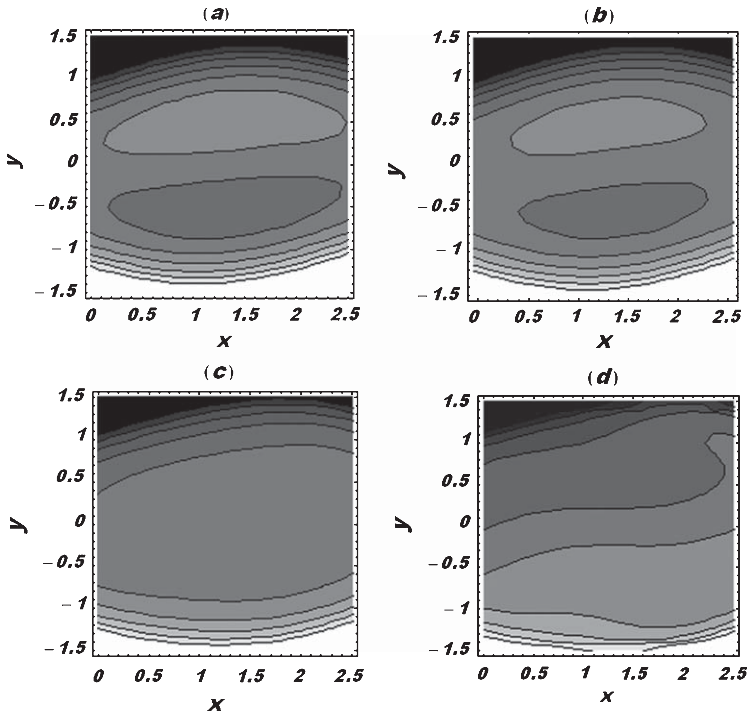

Fig. 20. Streamlines for $a = 0.4$, $b = 0.4$, $d = 1$, $\mathrm{Re} = 10$, $Fr = 1$, $\phi = \pi/6$, $\beta = 0.01$, $\sin\alpha = 0.2$, $dp^{(2)}/dx = 1$, $\theta = 1.4$ with different Γ (a) $\Gamma = 0.00$, (b) $\Gamma = 0.1$, (c) $\Gamma = 0.2$, (d) $\Gamma = 0.3$.

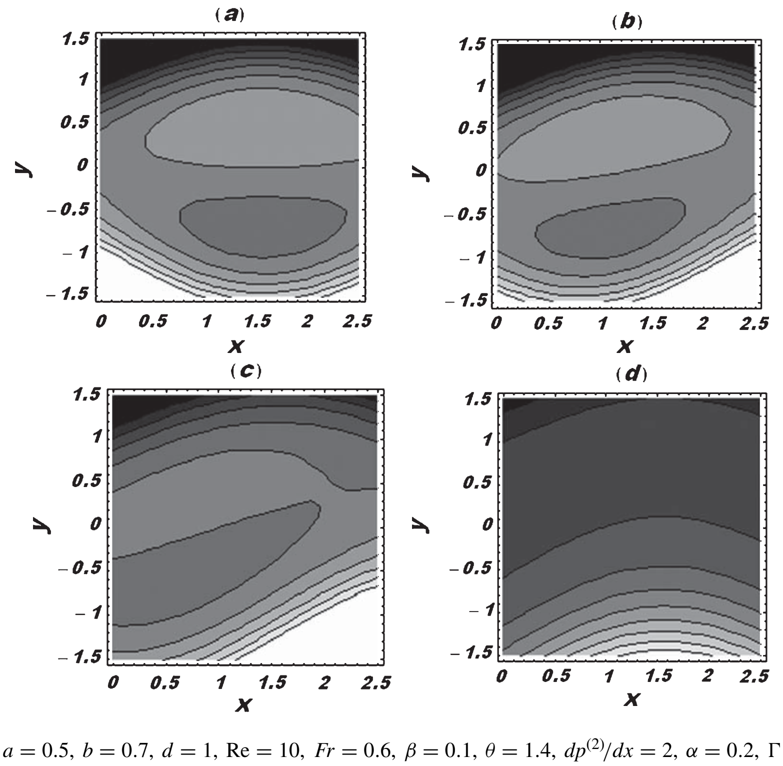

Fig. 21. Streamlines for $a = 0.5$, $b = 0.7$, $d = 1$, $\mathrm{Re} = 10$, $Fr = 0.6$, $\beta = 0.1$, $\theta = 1.4$, $dp^{(2)}/dx = 2$, $\alpha = 0.2$, $\Gamma = 0.01$ with different ϕ (a) $\phi = 0$, (b) $\phi = \pi/4$, (c) $\phi = \pi/2$, (d) $\phi = \pi$.

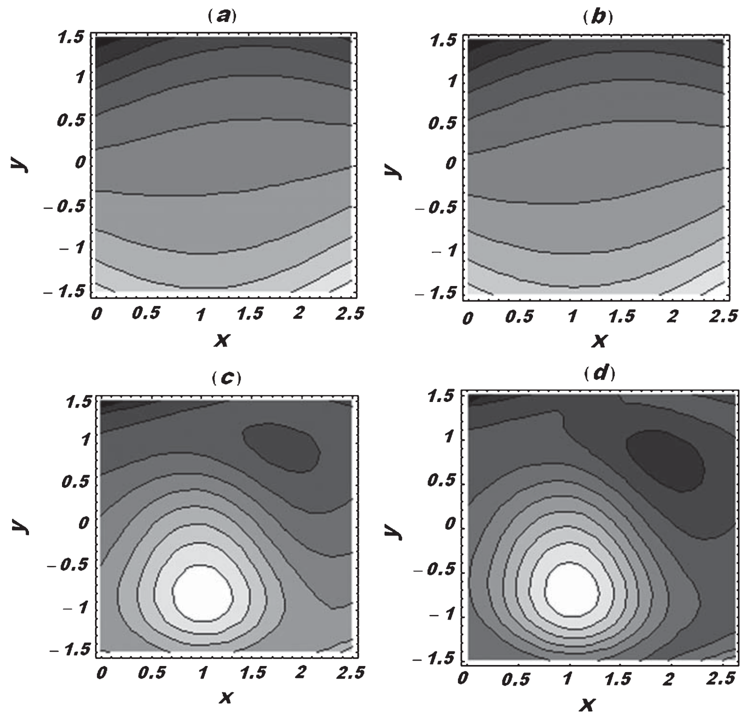

Fig. 22. Streamlines for $a = 0.5$, $b = 0.7$, $d = 1$, $\mathrm{Re} = 10$, $Fr = 1$, $\beta = 0.1$, $\theta = 0.5$, $dp^{(2)}/dx = 1.2$, $\phi = \pi/6$, $\Gamma = 0.01$ with different $\sin\alpha$ (a) $\sin\alpha = 0$, (b) $\sin\alpha = 0.4$, (c) $\sin\alpha = 0.8$, (d) $\sin\alpha = 1.2$.

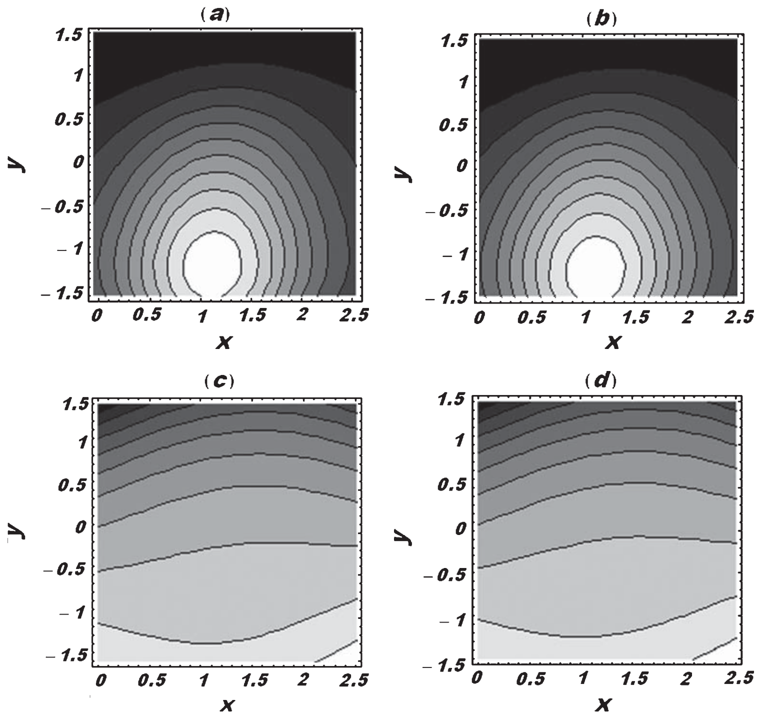

Fig. 23. Streamlines for $a = 0.5$, $b = 0.7$, $d = 2$, $\mathrm{Re} = 10$, $\alpha = 0.3$, $\beta = 0.1$, $\theta = 1.35$, $dp^{(2)}/dx = 1.2$, $\phi = \pi/6$, $\Gamma = 0.1$ with different Fr (a) $Fr = 1$, (b) $Fr = 2$, (c) $Fr = 3$, (d) $Fr = 4$.

While for an appropriately chosen $\Delta p_{\lambda}^{(2)} < 30$, the pumping rate decreases with an increase in Deborah number Γ. The effect of inclined angle α on pumping characteristics is plotted in Fig. 4. It is observed that the pumping rate and the pressure rise increase by increasing $\sin\alpha$. The variation of $\Delta p_{\lambda}^{(2)}$ with $\theta^{(2)}$ for different values of Froud number Fr is shown in Fig. 5. It is found that the pumping rate and the pressure rise decrease when Froud number Fr increases. The effect of phase difference ϕ on variation of $\Delta p_{\lambda}^{(2)}$ with $\theta^{(2)}$ is depicted in Fig. 6. We found that for sufficiently large values of $\Delta p_{\lambda}^{(2)}$, e.g. if $\Delta p_{\lambda}^{(2)} > 30$, the pumping rate decreases with an increase of phase difference ϕ and the pumping curves coincides with each other when $\Delta p_{\lambda}^{(2)} = 30$. Therefore, for an appropriately chosen $\Delta p_{\lambda}^{(2)} < 30$, the pumping rate increases with an increase in phase difference ϕ. The effect of channel width d on $\Delta p_{\lambda}^{(2)}$ with $\theta^{(2)}$ is illustrated in Fig. 7. For sufficiently large values of $\Delta p_{\lambda}^{(2)}$, e.g. $\Delta p_{\lambda}^{(2)} > 10$, the pumping rate decreases by increasing d and the pumping curves coincide with each other for $\Delta p_{\lambda}^{(2)} = 10$. Hence for an appropriately chosen $\Delta p_{\lambda}^{(2)} < 10$, the pumping rate increases when d increases. In Fig. 8 we have computed the pressure rise required to produce a zero average flow rate $\Delta p_{\lambda(\max)}^{(2)}$ as a function of d for different values of Deborah number Γ. For a fourth-grade fluid ($\Gamma \neq 0$), the value of $\Delta p_{\lambda(\max)}^{(2)}$ is larger than a viscous fluid ($\Gamma = 0$). The maximum pressure rise decreases with increasing d. Figure 9 is a graph of $\Delta p_{\lambda(\max)}^{(2)}$ versus the upper wave amplitude a for different values of inclined angle α. We noted that the maximum pressure rise increases as a and $\sin\alpha$ increase. Figure 10 plots $\Delta p_{\lambda(\max)}^{(2)}$ versus the lower wave amplitude b for different values of Froud number Fr. Here the maximum pressure rise increases as b increases and it decreases when Fr increases. The effect of phase difference ϕ on $\Delta p_{\lambda(\max)}^{(2)}$ with Re is presented in Fig. 11. This figure indicates that $\Delta p_{\lambda(\max)}^{(2)}$ decreases with an increase of ϕ and increases with an increase in Re.

4.2. Velocity behavior

Figure 12 plots the effects of β on the longitudinal velocity u. This figure shows that an increase in β leads

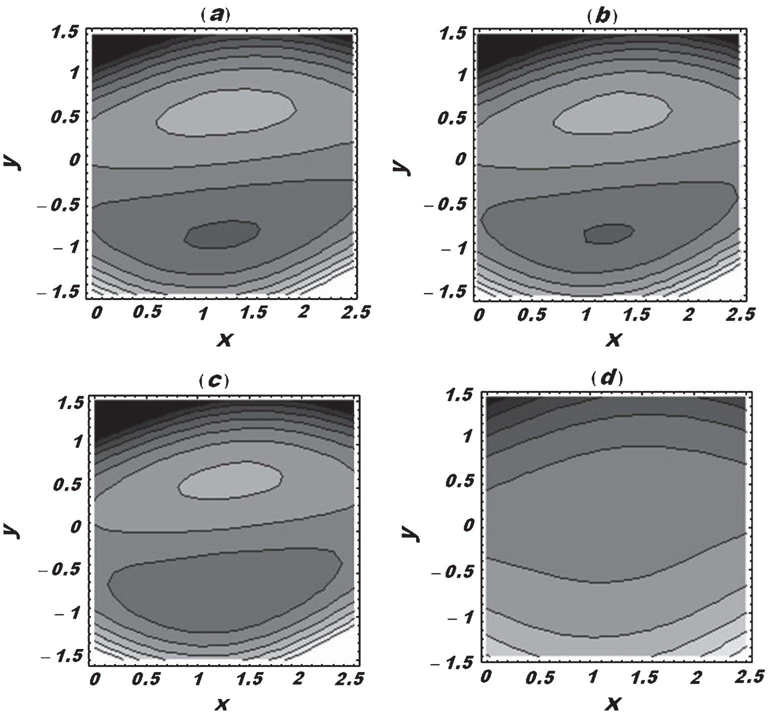

Fig. 24. Streamlines for $a = 0.5$, $b = 0.7$, $d = 1$, $\mathrm{Re} = 10$, $\alpha = 0.3$, $Fr = 1$, $\theta = 1.5$, $dp^{(2)}/dx = 1.2$, $\phi = \pi/6$, $\Gamma = 0.01$ with different β (a) $\beta = 0$, (b) $\beta = 0.05$, (c) $\beta = 0.1$, (d) $\beta = 0.9$.

to a decrease in the magnitude of u at the boundaries of the channel. However at the centre of the channel the magnitude of u increases when β increases. Figures 13 and 14 witness that there is a decrease in the magnitude of u at the boundaries of the channel when Γ and Fr are increased. At the centre of channel, an increase in the magnitude of u is noticed with an increase in Γ and Fr. Figure 15 depicts that an increase in Re causes an increase in the magnitude of u at the boundaries of the channel where at the centre of the channel, the magnitude of u decreases by increasing Re. Figure 16 shows that an increase in $\sin\alpha$ leads to a decrease in the magnitude of u at the boundaries of the channel. For channel centre there is an increase in the magnitude of u with an increase in $\sin\alpha$.

4.3. Concentration field

Figures 17 and 19 represents the concentration distribution for the different parameters. These figures display concentration distribution for various values of Sc and β_1. It is noticed that concentration field decreases with an increase in Sc and β_1. Figure 18 shows the concentration field increases in view of increasing values of chemical reaction parameter γ.

4.4. Trapping

The formation of an internally circulating bolus of fluid by closed streamlines is called trapping and this trapped bolus is pushed ahead along with the peristaltic wave. The effect of Γ on trapping is illustrated in Fig. 20. It is worthmentioning to note that the size of trapped bolus decreases by increasing Γ and disappears when $\Gamma = 0.2$. The streamlines for different ϕ are shown in Fig. 21. It is clear that the bolus appearing at the center region for $\phi = 0$ and it moves towards left and decreases in size as ϕ increases and disappears when $\phi = \pi$. The streamlines for different α are shown in Fig. 22. The trapped bolus does not exist for $\sin\alpha = 0$, but the trapping exists when $\sin\alpha \neq 0$ and the bolus volume increases by increasing $\sin\alpha$. The streamlines for different Fr have been displayed in Fig. 23. It is observed that the size of trapped bolus decreases with increasing Fr and disappears when $Fr = 3$. Effect of β on the trapping is plotted in Fig. 24. Here the size of trapped bolus decreases with increasing β and disappears for $\beta = 0.9$.

5. Concluding remarks

In this work the effects of slip condition on the peristaltic flow of fourth grade fluid in an inclined asymmetric channel with chemical reaction are analyzed subject to long wavelength and low Reynolds number approximation. The effects of slip parameters β and β_1 on pumping characteristics, longitudinal velocity, trapping and concentration are discussed in detail. The main points can be summed up as follows.

- The peristaltic pumping rate decreases by increasing β. However in copumping, the pumping rate increases by increasing β.
- The maximum pressure against which the peristaltic work as a pump decreases by increasing β.
- The size of trapped bolus above (below) the centre line increases (decreases) by increasing β.
- The magnitude of the longitudinal velocity decreases at the boundaries by increasing β. However it increases by increasing β at the centre of channel.
- With an increase in chemical reaction parameter γ, the concentration field increases.
- Concentration field decreases with an increase in Sc and concentration slip parameter β_1.

Appendix A

Here we provide the quantities appearing in the flow analysis.

$$R_1 = \frac{-2(F_0 + h_1 - h_2)}{(h_1 - h_2)^2(h_1 - h_2 + 6\beta)},$$

$$R_2 = \frac{3(F_0 + h_1 - h_2)(h_1 + h_2)}{(h_1 - h_2)^2(h_1 - h_2 + 6\beta)},$$

$$R_3 = \frac{-h_1^3 - 6F_0h_1h_2 - 3h_1^2h_2 + 3h_1h_2^2 + h_2^3 + 6F_0(h_1 - h_2)\beta}{(h_1 - h_2)^2(h_1 - h_2 + 6\beta)},$$

$$R_4 = \frac{-(h_1 + h_2)(2h_1h_2(-h_1 + h_2) + F_0(h_1^2 - 4h_1h_2 + h_2^2 + 6(h_1 - h_2)\beta))}{2(h_1 - h_2)^2(h_1 - h_2 + 6\beta)}.$$

$$M_1 = \frac{-1}{10}\left(\frac{dp_0}{dx} - 12G\right)^3, \quad M_2 = -\left(\frac{dp_0}{dx} - 12G\right)^2 R_2,$$

$$M_3 = \frac{-20F_1 + \left(\frac{dp_0}{dx} - 12G\right)^3 L_1 + \left(\frac{dp_0}{dx} - 12G\right)^2 R_2L_2 + \left(\frac{dp_0}{dx} - 12G\right) R_2^2L_3}{10(h_1 - h_2)^2(h_1 - h_2 + 6\beta)},$$

$$M_4 = \frac{L_4 + \left(\frac{dp_0}{dx} - 12G\right) R_2^2L_5 + \left(\frac{dp_0}{dx} - 12G\right)^3 L_6 + \left(\frac{dp_0}{dx} - 12G\right)^2 R_2L_7 + R_2^3L_8}{5(h_1 - h_2)^2(h_1 - h_2 + 2\beta)(h_1 - h_2 + 6\beta)},$$

$$M_5 = \frac{L_9 + R_2^3L_{10} + \left(\frac{dp_0}{dx} - 12G\right)^2 R_2L_{11} + \left(\frac{dp_0}{dx} - 12G\right) R_2^2L_{12} + \left(\frac{dp_0}{dx} - 12G\right)^3 L_{13}}{10(h_1 - h_2)^2(h_1 - h_2 + 2\beta)(h_1 - h_2 + 6\beta)},$$

$$M_6 = \frac{L_{14} + R_2^3L_{16} + \left(\frac{dp_0}{dx} - 12G\right)^2 R_2L_{18} + \left(\frac{dp_0}{dx} - 12G\right) R_2^2L_{15} + \left(\frac{dp_0}{dx} - 12G\right)^3 L_{17}}{10(h_1 - h_2)^2(h_1 - h_2 + 2\beta)(h_1 - h_2 + 6\beta)},$$

$$L_1 = (h_1 - h_2)^3(3h_1^2 + 4h_1h_2 + 3h_2^2),$$

$$L_2 = 20(h_1 - h_2)^3(h_1 + h_2),$$

$$L_3 = -240(h_1 - h_2)^2\beta,$$

$$L_4 = 15F_1(h_1 + h_2)(h_1 - h_2 + 2\beta),$$

$$L_5 = 120(h_1 - h_2)^3(h_1 + h_2)\beta,$$

$$L_6 = -(h_1 - h_2)^4(h_1 + h_2)[h_1^2 + 3h_1(h_2 - \beta) + h_2(h_2 + 3\beta)],$$

$$L_7 = 5(h_1 - h_2)^3[-(h_1 - h_2)(h_1^2 + 4h_1h_2 + h_2^2) + 6(h_1^2 + h_2^2)\beta],$$

$$L_8 = -80(h_1 - h_2)^2\beta(h_1 - h_2 + 6\beta),$$

$$L_9 = -60F_1(h_1 - h_2 + 2\beta)[h_1(h_2 - \beta) + h_2\beta],$$

$$L_{10} = 160(h_1 - h_2)^2(h_1 + h_2)\beta(h_1 - h_2 + 6\beta),$$

$$L_{11} = 20(h_1 - h_2)^2(h_1 + h_2)[h_1h_2(h_1 - h_2)^2 - (h_1 - h_2)(h_1 + h_2)^2\beta + 6(h_1^2 + h_2^2)\beta^2],$$

$$L_{12} = 240(h_1 - h_2)^2\beta[-h_1h_2(h_1 - h_2) + 2(h_1^2 + h_1h_2 + h_2^2)\beta],$$

$$L_{13} = (h_1 - h_2)^2[h_1h_2(h_1 - h_2)^2(4h_1^2 + 7h_1h_2 + 4h_2^2) - 2(h_1 - h_2)(2h_1^4 + 3h_1^3h_2 + 3h_1h_2^3 + 2h_2^4)\beta$$
$$+12(h_1^4 + h_1^3h_2 + h_1^2h_2^2 + h_1h_2^3 + h_2^4)\beta^2],$$
$$L_{14} = -5F_1(h_1 + h_2)(h_1 - h_2 + 2\beta)[h_1^2 - 4h_1h_2 + h_2^2 + 6(h_1 - h_2)\beta],$$
$$L_{15} = -480h_1h_2(h_1 - h_2)^2(h_1 + h_2)\beta^2,$$
$$L_{16} = -160h_1h_2(h_1 - h_2)^2\beta(h_1 - h_2 + 6\beta),$$
$$L_{17} = 2h_1h_2(h_1 - h_2)^2[-h_1h_2(h_1 - h_2)^2(h_1 + h_2) + 2(h_1 - h_2)(h_1^3 + h_2^3)\beta - 6(h_1 + h_2)(h_1^2 + h_2^2)\beta^2],$$
$$L_{18} = 10h_1h_2(h_1 - h_2)^2[-h_1h_2(h_1 - h_2)^2 + 2(h_1 - h_2)(h_1^2 + h_2^2)\beta - 12(h_1^2 + h_1h_2 + h_2^2)\beta^2],$$
$$L_{19} = 3(h_1 - h_2)^3(3h_1^2 + 4h_1h_2 + 3h_2^2),$$
$$L_{20} = 60(h_1 - h_2)^3(h_1 + h_2),$$
$$L_{21} = 120(h_1 - h_2)^3,$$
$$L_{22} = (h_1 - h_2)^3[500h_1^4M_1 + 16h_1^3(50h_2M_1 + 21M_2) + 9h_1^2(100h_2^2M_1 + 56h_2M_2 + 21M_3)$$
$$+h_2(500h_2^3M_1 + 336h_2^2M_2 + 189h_2M_3 + 70M_4) + h_1(800h_2^3M_1 + 504h_2^2M_2 + 252h_2M_3 + 70M_4)],$$
$$L_{23} = 840(h_1 - h_2)^2[(h_1 - h_2)((3h_1^2 + 4h_1h_2 + 3h_2^2)M_1 + 2(h_1 + h_2)M_2) - 6M_3\beta],$$
$$L_{24} = 56(h_1 - h_2)^2[(h_1 - h_2)(40M_1(h_1^3 + h_2^3) + 60h_1h_2M_1(h_1 + h_2) + 27M_2(h_1^2 + h_2^2)$$
$$36h_1h_2M_1 + 15M_3(h_1 + h_2)) - 30M_4\beta],$$
$$L_{25} = 105F_2(h_1 + h_2)(h_1 - h_2 + 2\beta),$$
$$L_{26} = -84(h_1 - h_2)^3[(h_1 - h_2)(4(h_1^2 + 3h_1h_2 + h_2^2)(5(h_1^2 + h_1h_2 + h_2^2)M_1 + 3(h_1 + h_2)M_2)$$
$$+5(h_1^2 + 4h_1h_2 + h_2^2)M_3 - 2(20h_1^4M_1 + h_1^3(-40h_2M_1 + 18M_2) - 3h_1^2(20h_2^2M_1 + 6h_2M_2 - 5M_3)$$
$$-2h_1(20h_2^3M_1 + 9h_2^2M_2 - 5M_4) + h_2(20h_2^3M_1 + 18h_2^2M_2 + 15h_2M_3 + 10M_4))\beta],$$
$$L_{27} = -(h_1 - h_2)^3[(h_1 - h_2)(200(h_1 + h_2)(2h_1^4 + 6h_1^3h_2 + 5h_1^2h_2^2 + 6h_1h_2^3 + 2h_2^4)M_1$$
$$+252(h_1^2 + h_1h_2 + h_2^2)(h_1^2 + 3h_1h_2 + h_2^2)M_2 + 126(h_1 + h_2)(h_1^2 + 3h_1h_2 + h_2^2)M_3$$
$$+35(h_1^2 + 4h_1h_2 + h_2^2)M_4) - 6(100h_1^5M_1 + h_1^4(-300h_2M_1 + 84M_2)$$
$$-3h_1h_2^2(100h_2^2M_1 + 56h_2M_2 + 21M_3) + h_1^3(-4h_2(125h_2M_1 + 42M_2) + 63M_3)$$
$$-h_1^2(500h_2^3M_1 + 252h_2^2M_2 + 63h_2M_3 - 35M_4) + h_2^2(100h_2^3M_1 + 84h_2^2M_2 + 63h_2M_3 + 35M_4))\beta],$$
$$L_{28} = 840(h_1 - h_2)^2[-(h_1 - h_2)^2(2(h_1 + h_2)(h_1^2 + 3h_1h_2 + h_2^2)M_1 + (h_1^2 + 4h_1h_2 + h_2^2)M_2)$$
$$+2(h_1 - h_2)(3(h_1^3M_1 + h_1^2(-h_2M_1 + M_2) + h_1(-h_2^2M_1 + M_3)$$
$$+h_2(h_2(h_2M_1 + M_2) + M_3)) - M_4)\beta - 12M_4\beta^2],$$
$$L_{29} = -210F_2(h_1 - h_2 + 2\beta)(h_1(h_2 - \beta) + h_2\beta),$$
$$L_{30} = 840(h_1 - h_2)^2[h_1h_2(h_1 - h_2)^2((4h_1^2 + 7h_1h_2 + 4h_2^2)M_1 + 2(h_1 + h_2)M_2)$$
$$-2(h_1 - h_2)(2h_1^4M_1 + 3h_1^2h_2M_2 + h_2^3(2h_2M_1 + M_2) + h_1^3(3h_2M_1 + M_2)$$
$$+3h_1h_2(h_2(h_2M_1 + M_2) + M_3) - (h_1 + h_2)M_4\beta + 12(h_1^4M_1 + h_1^3(h_2M_1 + M_2)$$
$$+h_1^2(h_2(h_2M_1 + M_2) + M_3) + (h_1 + h_2)(h_2(h_2(h_2M_1 + M_2) + M_3) + M_4))\beta^2],$$

$$
\begin{aligned}
L_{31} &= 168(h_1-h_2)^2[h_1h_2(h_1-h_2)^2(20h_1^3M_1+4h_1^2(10h_2M_1+3M_2)+h_1(40h_2^2M_1+21h_2M_2+5M_3)\\
&\quad +h_2(4h_2(5h_2M_1+3M_2)+5M_3))-(h_1-h_2)(20h_1^5M_1+4h_1^4(5h_2M_1+3M_2)\\
&\quad +h_1^3(-20h_2^2M_1+18h_2M_2+5M_3)+h_2^3(4h_2(5h_2M_1+3M_2)+5M_3)-5h_1^2(4h_2^3M_1-3h_2M_3)\\
&\quad +h_1h_2(20h_2^3M_1+18h_2^2M_2+15h_2M_3+10M_4))\beta+2(20h_1^5M_1+2h_1^4(10h_2M_1+9M_2)\\
&\quad +h_1^3(20h_2^2M_1+18h_2M_2+15M_3)+(h_1^2+h_1h_2+h_2^2)(20h_2^3M_1+18h_2^2M_2+15h_2M_3+10M_4))\beta^2],\\
L_{32} &= (h_1-h_2)^2[h_1h_2(h_1-h_2)^2(800h_1^4M_1+4h_1^3(425h_2M_1+126M_2)\\
&\quad +4h_1^2(500h_2^2M_1+252h_2M_2+63M_3)+2h_2(400h_2^3M_1+252h_2^2M_2+126h_2M_3+35M_4)\\
&\quad +h_1(h_2(4h_2(425h_2M_1+252M_2)+441M_3)+70M_4))-2(h_1-h_2)(400h_1^6M_1\\
&\quad +12h_1^5(25h_2M_1+21M_2)+h_1^4(-600h_2^2M_1+252h_2M_2+126M_3)\\
&\quad +h_1^3(-9h_2(4h_2(25h_2M_1+7M_2)-21M_3)+35M_4)\\
&\quad +3h_1h_2^2(100h_2^3M_1+84h_2^2M_2+63h_2M_3+35M_4)+h_2^3(400h_2^3M_1+252h_2^2M_2+126h_2M_3+35M_4)\\
&\quad -3h_1^2(200h_2^4M_1+84h_2^3M_2-35h_2M_4))\beta+12(100h_1^6M_1+4h_1^5(25h_2M_1+21M_2)\\
&\quad +h_1^4(100h_2^2M_1+84h_2M_2+63M_3)+(h_1^3+h_1^2h_2+h_1h_2^2+h_2^3)\\
&\quad \times(100h_2^3M_1+84h_2^2M_2+63h_2M_3+35M_4))\beta^2],\\
L_{33} &= -35F_2(h_1+h_2)(h_1-h_2+2\beta)(h_1^2-4h_1h_2+h_2^2+6(h_1-h_2)\beta),\\
L_{34} &= 1680h_1h_2(h_1-h_2)^2[-h_1h_2(h_1-h_2)^2(2(h_1+h_2)M_1+M_2)+2(h_1-h_2)(2(h_1^3+h_2^3)M_1\\
&\quad +(h_1^2+h_2^2)M_2-M_4)\beta-12(h_1^3M_1+h_1^2(h_2M_1+M_2)+(h_1(h_2(h_2M_1+M_2)+M_3)\\
&\quad +h_2(h_2(h_2M_1+M_2)+M_3)+M_4))\beta^2],\\
L_{35} &= 56h_1h_2(h_1-h_2)^2[-h_1h_2(h_1-h_2)^2(20(3h_1^2+4h_1h_2+3h_2^2)M_1+36(h_1+h_2)M_2+15M_3)\\
&\quad +2(h_1-h_2)(20(3h_1^4-h_1^2h_2^2+3h_2^4)M_1+36(h_1^3+h_2^3)M_2+15(h_1^2+h_2^2)M_3)\beta\\
&\quad -12(20h_1^4M_1+2h_1^3(10h_2M_1+9M_2)+h_1^2(20h_2^2M_1+18h_2M_2+15M_3)+(h_1+h_2)\\
&\quad \times(20h_2^3M_1+18h_2^2M_2+15h_2M_3+10M_4))\beta^2],\\
L_{36} &= 2h_1h_2(h_1-h_2)^2[-h_1h_2(h_1-h_2)^2(200(h_1+h_2)(2h_1^2+h_1h_2+2h_2^2)M_1\\
&\quad +84(3h_1^2+4h_1h_2+3h_2^2)M_2+126(h_1+h_2)M_3+35M_4)\\
&\quad +2(h_1-h_2)(200(2h_1^5-h_1^3h_2^2-h_1^2h_2^3+2h_2^5)M_1+84(3h_1^4-h_1^2h_2^2+3h_2^4)M_2\\
&\quad +126(h_1^3+h_2^3)M_3+35(h_1^2+h_2^2)M_4)\beta-12(100h_1^5M_1+4h_1^4(25h_2M_1+21M_2)\\
&\quad +h_1^3(100h_2^2M_1+84h_2M_2+63M_3)+(h_1^2+h_1h_2+h_2^2)\\
&\quad \times(100h_2^3M_1+84h_2^2M_2+63h_2M_3+35M_4))\beta^2],\\
L_{37} &= 6(h_1-h_2)^3[500h_1^4M_1+16h_1^3(50h_2M_1+21M_2)+9h_1^2(100h_2^2M_1+56h_2M_2+21M_3)\\
&\quad +h_2(500h_2^3M_1+336h_2^2M_2+189h_2M_3+70M_4)+h_1(800h_2^3M_1+504h_2^2M_2+252h_2M_3+70M_4)],\\
L_{38} &= 336(h_1-h_2)^3[40M_1(h_1^3+h_2^3)+60M_1(h_1^2h_2+h_1h_2^2)\\
&\quad +9M_2(3h_1^2+4h_1h_2+3h_2^2)+15(h_1+h_2)M_3+5M_4],\\
L_{39} &= 5040(h_1-h_2)^3[(3h_1^2+4h_1h_2+3h_2^2)M_1+2(h_1+h_2)M_2+M_3],
\end{aligned}
$$

$$N_1 = \frac{-20}{7} M_1 \left(\frac{dp_0}{dx} - 12G \right)^2,$$

$$N_2 = \frac{-4}{5} \left(\frac{dp_0}{dx} - 12G \right) \left(3M_2 \left(\frac{dp_0}{dx} - 12G \right) + 20M_1 R_2 \right),$$

$$N_3 = \frac{-3}{5} \left(3M_3 \left(\frac{dp_0}{dx} - 12G \right)^2 + 8R_2 \left(3M_2 \left(\frac{dp_0}{dx} - 12G \right) + 5M_1 R_2 \right) \right),$$

$$N_4 = -M_4 \left(\frac{dp_0}{dx} - 12G \right)^2 - 12R_2 \left(M_3 \left(\frac{dp_0}{dx} - 12G \right) + 2M_2 R_2 \right),$$

$$N_5 = \frac{-70F_2 + \left(\frac{dp_0}{dx} - 12G \right)^2 L_{22} + R_2^2 L_{23} + \left(\frac{dp_0}{dx} - 12G \right) R_2 L_{24}}{35(h_1 - h_2)^2 (h_1 - h_2 + 6\beta)},$$

$$N_6 = \frac{L_{25} + \left(\frac{dp_0}{dx} - 12G \right) R_2 L_{26} + \left(\frac{dp_0}{dx} - 12G \right)^2 L_{27} + R_2^2 L_{28}}{35(h_1 - h_2)^2 (h_1 - h_2 + 2\beta)(h_1 - h_2 + 6\beta)},$$

$$N_7 = \frac{L_{29} + \left(\frac{dp_0}{dx} - 12G \right) R_2 L_{31} + \left(\frac{dp_0}{dx} - 12G \right)^2 L_{32} + R_2^2 L_{30}}{35(h_1 - h_2)^2 (h_1 - h_2 + 2\beta)(h_1 - h_2 + 6\beta)},$$

$$N_8 = \frac{L_{33} + \left(\frac{dp_0}{dx} - 12G \right) R_2 L_{35} + \left(\frac{dp_0}{dx} - 12G \right)^2 L_{36} + R_2^2 L_{34}}{70(h_1 - h_2)^2 (h_1 - h_2 + 2\beta)(h_1 - h_2 + 6\beta)}.$$

Acknowledgments

First author appreciates the support of Global Research Network for Computational Mathematics and King Saud University of Saudi Arabia for this research.

References

[1] Y. Abd elmaboud and Kh.S. Mekheimer, Non-linear peristaltic transport of a second-order fluid through a porous medium, *App Math Model* **35** (2011), 2695.

[2] N. Ali, Q. Hussain, T. Hayat and S. Asghar, Slip effects on the peristaltic transport of MHD fluid with variable viscosity, *Phys Lett A* **372** (2008), 1477.

[3] C. Derek, D.C. Tretheway and C.D. Meinhart, Apparent fluid slip athydrophobic microchannel walls, *Phys Fluids* **14** (2002), L9.

[4] A. Ebaid, Effect of magnetic field and wall slip conditions on the peristaltic transport of a Newtonian fluid in an asymmetric channel, *Phys Lett A* **372** (2008), 4493.

[5] T. Hayat and F.M. Abbasi, Variable viscosity effects on the peristaltic motion of a third-order fluid, *Int J Numer Meth Fluids*, doi: 10.1002/fld.2428.

[6] T. Hayat, Z. Asghar, S. Asghar and S. Mesloub, Influence of inclined magnetic field on peristaltic transport of fourth grade fluid in an inclined asymmetric channel, *J Taiwan Institute of Chemical Engineers* **41** (2010), 553.

[7] T. Hayat, S. Hina and N. Ali, Simultaneous effects of slip and heat transfer on the peristaltic flow, *Comm Nonlinear Sci Numer Simul* **15** (2010), 1526.

[8] M. Kothandapani and S. Srinivas, Peristaltic transport of a Jeffrey fluid under the effect of magnetic field in an asymmetric channel, *Int J Non-Linear Mech* **43** (2008), 915.

[9] T.W. Latham, Fluid motion in a peristaltic pump, M.S. Thesis, MIT, Cambridge, 1966.

[10] Kh.S Mekheimer and Y. Abd elmaboud, Peristaltic flow of a couple stress fluid in an annulus: Application of an endoscope, Physica A, *Statistical Mech and its Appli* **387** (2008), 2403.

[11] Kh.S. Mekheimer and Y. Abd elmaboud, The influence of heat transfer and magnetic field on peristaltic transport of a Newtonian fluid in a vertical annulus: Application of an endoscope, *Phys Lett A* **372** (2008), 1657.

[12] S. Nadeem and Noreen Sher Akbar, Influence of heat and chemical reaction on Walter's B fluid model for blood flow through a tapered artery, *J Taiwan Institute of Chemical Engineers* **42** (2011), 67.

[13] S. Nadeem and Safia Akram, Slip effects on the peristaltic flow of a Jeffrey fluid in an asymmetric channel under the effect of induced magnetic field, *Int J Numer Meth Fluids* **63** (2010), 374.

[14] S.K. Pandey and D. Tripathi, Influence of magnetic field on the peristaltic flow of a viscous fluid through a finite-length cylindrical tube, *App Bionics and Biomech* **7** (2010), 169.
[15] S. Srinivas and M. Kothandapani, The influence of heat and mass transfer on MHD peristaltic flow through a porous space with compliant walls, *App Math and Comp* **213** (2009), 197.
[16] S. Srinivas and R. Muthuraj, Peristaltic transport of a Jeffrey fluid under the effect of slip in an inclined asymmetric channel, *Int J Applied Mech* **2** (2010), 437.
[17] D. Tripathi, S.K. Pandey and S. Das, Peristaltic flow of viscoelastic fluid with fractional Maxwell model through a channel, *App Math Comp* **215** (2010), 3645.